

Crystalline phases in chiral ferromagnets: Destabilization of helical order

Inga Fischer,¹ Nayana Shah,² and Achim Rosch¹

¹*Institute for Theoretical Physics, University of Cologne, 50937 Cologne, Germany*

²*Department of Physics, University of Illinois at Urbana-Champaign, 1110 West Green Street, Urbana, Illinois 61801, USA*

(Received 30 July 2007; published 15 January 2008)

In chiral ferromagnets, weak spin-orbit interactions twist the ferromagnetic order into spirals, leading to helical order. We investigate an extended Ginzburg-Landau theory of such systems where the helical order is destabilized in favor of crystalline phases. These crystalline phases are based on periodic arrangements of double-twist cylinders and are strongly reminiscent of blue phases in liquid crystals. We discuss the relevance of such blue phases for the phase diagram of the chiral ferromagnet MnSi.

DOI: [10.1103/PhysRevB.77.024415](https://doi.org/10.1103/PhysRevB.77.024415)

PACS number(s): 75.10.-b, 75.30.Kz, 75.90.+w

I. INTRODUCTION

In metallic magnets without inversion symmetry—so-called chiral ferromagnets—spin-orbit coupling effects determine the physics decisively: they can twist the magnetization into a helix in the ordered phase of the material. Prominent examples are MnSi and FeGe, which have been known for a long time to exhibit spiral order.¹ Recently, interest in such materials has been renewed with a number of experiments that, on the one hand, found non-Fermi liquid behavior in a large temperature and pressure region of the phase diagram² and, on the other hand, uncovered signs of a peculiar partially ordered state in neutron scattering experiments.³

In the ordered state of MnSi, helical order is observed in neutron scattering experiments in the form of Bragg peaks situated on a sphere in reciprocal space. The radius of this sphere is proportional to the inverse pitch of the helix, and the peaks are positioned in the $\langle 111 \rangle$ directions. This locking of the helices is due to higher-order spin-orbit coupling effects. For temperatures down to 12 K, the phase diagram exhibits a second-order phase transition out of the helical into the disordered, isotropic phase when external pressure is applied. Below 12 K, helical order is lost at external pressure of 12–14 kbars via a first-order phase transition into a “partially ordered” state. This state seems to retain remnants of helical order on intermediate time and length scales: neutron scattering experiments reveal a signal on the surface of a sphere in reciprocal space, which is resolution limited in the radial direction but smeared out over the surface of the sphere.³ Maxima of the signal now point into the $\langle 110 \rangle$ directions but are no longer sharply peaked.

Motivated by these experiments, we investigated ways of destabilizing helical order in chiral ferromagnets and the possible new phases that can exist besides helical order. Such phases are well known for cholesteric liquid crystals,⁴ i.e., chiral nematics, where several so-called blue phases have been observed. In these phases (more precisely, in phases I and II), crystalline order is formed, which can be interpreted as a periodic network of ordered cylinders, see below. The lattice spacing is often of the order of a few hundred nanometers, leading to the colorful appearance of these phases (including the color blue in some variants).

As the Ginzburg-Landau theory for the director of a chiral nematic liquid is very similar to that for the vector order

parameter of a chiral magnet (see discussion below), the question arises whether similar phases are realized in magnetic systems. This question has been addressed in some detail by Wright and Mermin⁴ many years ago. They showed that amplitude fluctuations, which are essential for the stability of blue phases, cost a factor of 3 more energy for ferromagnets compared to liquid crystals and concluded that such phases do not appear within a Ginzburg-Landau theory with local interactions.

Motivated by the physics of MnSi, several groups have reexamined this issue. Rößler *et al.*⁵ added a further parameter to the Ginzburg-Landau theory, allowing them to reduce the energy of amplitude fluctuations arguing that such a term might arise from higher-order fluctuation corrections. The term considered in Ref. 5 is, however, nonanalytic in the Ginzburg-Landau order parameter. In the presence of such a term, they were able to show that a crystalline array of cylinders can have lower energy than a uniform helix. We will discuss a similar structure below. An alternative route (also followed by us) to destabilize the helical solution are nonlocal interactions, as suggested by Binz *et al.*⁶ They considered crystals formed from superpositions of helices to be responsible for the partially ordered phase of MnSi.

As pointed out by Wright and Mermin,⁴ it is useful to distinguish two rather different limits when investigating the physics of blue phases. Here, one has to compare the correlation length ξ for amplitude fluctuations of the ordered state (i.e., the width of a typical domain wall) with the wavelength $2\pi/q_0$ of the helical state. For $\xi q_0 \gg 1$ (the high-chirality limit), the magnetic structure can be described by a superposition of a few helices. This approach was taken by Binz *et al.*⁶

The factor ξq_0 is proportional to the strength of spin-orbit coupling,¹ and therefore expected to become large only very close to the second-order phase transition where ξ diverges. As the pitch of the helix³ in MnSi, $2\pi/q_0 \approx 175$ Å, is very large compared to all other microscopic length scales, we think that the low-chirality limit ($\xi q_0 \ll 1$) is more appropriate for the description of the high-pressure phase of this material. In this limit, amplitude fluctuations of the order parameter cost more energy than twists of the phase and, therefore, one has to look for order-parameter configurations with as little amplitude fluctuations as possible.

In the following, we will first investigate which terms in the Ginzburg-Landau theory destabilize the helical state.

Then, we will suggest variational solutions appropriate in the low-chirality limit. Finally, we investigate experimental consequences of the resulting structures.

II. CHIRAL MAGNETS AND BLUE PHASES

The starting point of our investigation is a Ginzburg-Landau theory at finite temperature, assuming that all modes with nonzero Matsubara frequencies are massive and can be integrated out.

Up to second order in spin-orbit coupling, the Ginzburg-Landau theory for chiral ferromagnets is given by¹

$$f(\mathbf{r}) = \frac{\alpha}{2} \sum (\nabla M_i)^2 + \gamma \mathbf{M} \cdot (\nabla \times \mathbf{M}) + f_{\text{FM}}, \quad (1)$$

where $\mathbf{M} = \mathbf{M}(\mathbf{r})$ is the position-dependent magnetization and $f_{\text{FM}} = \frac{\delta}{2}(\mathbf{M})^2 + u(\mathbf{M})^4$ is the Landau free energy of the underlying ferromagnet. Spin-orbit coupling is present in the form of the Dzyaloshinsky-Moriya interaction $\propto \gamma$. In order to facilitate the following discussion, we also provide a second form for Eq. (1). It can be rewritten by setting $\mathbf{M} = \lambda \hat{n}$, where λ is the amplitude and \hat{n} is the direction of the magnetization \mathbf{M} :

$$f(\mathbf{r}) = \frac{\alpha}{2} \lambda^2 \left(\nabla_i n_j + \frac{\gamma}{\alpha} \varepsilon_{ijk} n_k \right)^2 + \frac{\alpha}{2} (\nabla \lambda)^2 - \frac{\gamma^2}{\alpha} \lambda^2 + f_{\text{FM}}(\lambda), \quad (2)$$

with $f_{\text{FM}}(\lambda) = \frac{\delta}{2} \lambda^2 + u \lambda^4$.

Terms that break rotational symmetry are of higher order in spin-orbit coupling and take the form, e.g.,

$$B_1 [(\partial_x M_x)^2 + (\partial_y M_y)^2 + (\partial_z M_z)^2] + B_2 [(\partial_x^2 \mathbf{M})^2 + (\partial_y^2 \mathbf{M})^2 + (\partial_z^2 \mathbf{M})^2] + B_3 (M_x^4 + M_y^4 + M_z^4) \quad (3)$$

(to fourth order in spin-orbit coupling) for the point group $P2_13$ of MnSi.⁷ These terms will be neglected for the moment.

The helical state

$$\hat{n}^{\text{helix}}(\mathbf{r}) = \hat{x} \cos(q_0 z) + \hat{y} \sin(q_0 z), \quad (4)$$

with $q_0 = \gamma/\alpha$, can be shown to be the lowest energy state of Eq. (1) if one assumes that the amplitude λ of the magnetization is constant and was argued in Ref. 4 to be the only ordered phase possible for chiral ferromagnets. Higher-order terms in the Ginzburg-Landau expansion can, however, serve to destabilize this helical order and induce other phases. The simplest (i.e., of lowest order in spin-orbit coupling) of these terms will be the focus of our investigation in this paper:

$$\left(\sum_i M_i \nabla M_i \right)^2 = \frac{1}{4} (\nabla \mathbf{M}^2)^2. \quad (5)$$

This term acts only on the amplitude of the magnetization, not on its direction. Therefore, it gives no contribution to the free energy density in the helical phase, which has a uniform amplitude. If Eq. (5) has a negative prefactor, then in a cer-

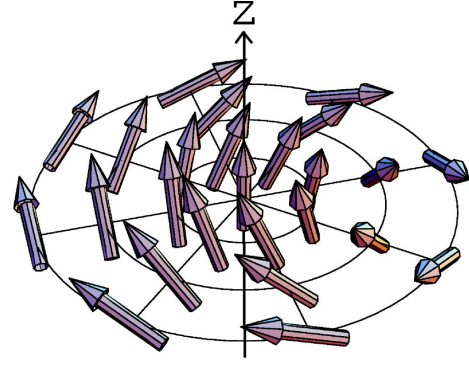


FIG. 1. (Color online) Cut through a double-twist cylinder: Double-twist-configuration of the magnetization. Sheets of constant magnetization are wrapped as cylinders around a common axis.

tain parameter regime, it can be expected to destabilize helical order in favor of an order parameter with a fluctuating amplitude. In the following, we will use the shorthand $(\mathbf{M} \nabla \mathbf{M})^2$ for expression (5).

In order to determine the new states that could be stabilized by Eq. (5), it is instructive to explore the close analogies between chiral ferromagnets and chiral liquid crystals.⁴ The order parameter of chiral liquid crystals is a director and, as a consequence, topological defects are fundamentally different in both systems. However, chiral liquid crystals can be described by a free energy density that is quite similar in form to Eq. (2), the only differences being an additional cubic term in λ and an extra factor 1/3 in front of the term $\propto (\nabla \lambda)^2$.

Locally, the blue phases are based on a configuration of the magnetization that can be shown to be even lower in energy than the helix:

$$\hat{n}^{\text{dt}}(\mathbf{r}) = \hat{z} \cos(qr) - \hat{\phi} \sin(qr), \quad (6)$$

in cylinder coordinates, see Fig. 1. This can be easily seen⁴ by comparing the energy density of the uniform helix, $-\frac{\gamma^2}{2\alpha} \lambda^2 + f_{\text{FM}}(\lambda)$, to the result obtained by plugging Eq. (6) into Eq. (2): For $\lambda = \text{const}$ and $q = q_0$, the first two terms in Eq. (2) vanish for $r=0$ and, therefore, the energy density at $r=0$ is given by $-\frac{\gamma^2}{2\alpha} \lambda^2 + f_{\text{FM}}(\lambda)$, i.e., lowered by an extra factor $-\frac{\gamma^2}{2\alpha} \lambda^2$.

This so-called double-twist configuration is cylindrically symmetric: sheets of constant magnetization are rolled up around a common cylinder axis (see Fig. 1). Configuration (6) is, however, only favored in the vicinity of the cylinder axis—the energy difference between the helix and the double-twist configuration diminishes and even becomes positive as the distance from the cylinder axis is increased. Isolated double-twist configurations, therefore, necessarily have to occur in the form of cylinders with an amplitude that becomes zero at a certain distance from the cylinder axis. However, amplitude fluctuations cost energy, as can be seen from the second term in Eq. (2). In the case of liquid crystals, the prefactor of $(\nabla \lambda)^2$ is small enough for double-twist cylinders to become energetically lower in energy than the helix

(see discussion above). Crystals made of these double-twist cylinders are indeed believed to lie at the heart of the blue phases I and II in liquid crystals.⁴ In the case of the ferromagnet, however, the energy cost of amplitude fluctuations outweighs the energy gains due to directional fluctuations within the double-twist structure and, for a free energy density given by Eq. (1) (single), double-twist cylinders do not occur.⁴

Adding term (5) to the free energy density can invalidate this conclusion: if the prefactor of Eq. (5) is allowed to become negative, it can reduce the cost of amplitude fluctuations and allow for the appearance of blue phases even in chiral ferromagnets. If Eq. (5) has a negative prefactor, then the inclusion of higher-order terms in the Ginzburg-Landau theory becomes necessary in order to obtain a stable solution and avoid, e.g., an unbounded magnetization.

In the following, we want to analyze the possible occurrence of the analog of blue phases in chiral ferromagnets. By rescaling the magnetization, the free energy density, and the momenta, the free energy density can be cast into the following form:

$$f(\mathbf{r}) = \delta \mathbf{M}^2 + \sum (\nabla M_i)^2 + \mathbf{M} \cdot (\nabla \times \mathbf{M}) + \mathbf{M}^4 + \xi (\mathbf{M} \nabla \mathbf{M})^2 + \eta h_i(\mathbf{M}), \quad (7)$$

where $\xi < 0$, $\eta > 0$, and $h_i(\mathbf{M})$ is a term containing k powers of \mathbf{M} and l derivatives ($k > 4$, $l \geq 2$), which is used to stabilize solutions against an unbounded magnetization and oscillations thereof. Possible choices are, for example, $h_1(\mathbf{M}) = (\mathbf{M} \nabla \mathbf{M})^2 \sum (\nabla M_i)^2$, $h_2(\mathbf{M}) = (\mathbf{M} \nabla \mathbf{M})^4$, and $h_3(\mathbf{M}) = \mathbf{M}^2 (\mathbf{M} \nabla \mathbf{M})^2$. In the rest of this paper, we will use $h_1(\mathbf{M})$ exclusively: this term is the one with the least number of derivatives and powers of \mathbf{M} that, on the one hand, stabilizes single double-twist cylinders and, on the other hand, is identically zero for the single helix.

III. FROM CYLINDERS TO CRYSTALS

As the first step, we investigated single double-twist cylinders for $\delta = 1/4$. At this point, the helical and isotropic phase are degenerate with $f^{\text{helical}} = f^{\text{isotropic}} = 0$. If a single cylinder can now be shown to have negative free energy, then the system can lower its free energy further by creating extended networks of double-twist cylinders: crystalline phases (the analogy to blue phases in liquid crystals) can be expected to form in chiral ferromagnets.

Setting $\mathbf{M} = \hat{n}^{\text{dt}}(\mathbf{r}) \lambda(r)$, with $\hat{n}^{\text{dt}}(\mathbf{r})$ given by Eq. (6), we calculated numerically the amplitude function $\lambda(r)$ that minimizes the free energy density [Eq. (7)] (for certain values of ξ and η), subject to the condition that the magnetization drops to zero at a certain distance from the cylinder axis. For a given η and sufficiently negative values of ξ , single cylinders are stable configurations within a Ginzburg-Landau theory of the form of Eq. (7), see Fig. 2. In order to minimize its free energy, the system will try to produce many such cylinders, packed as tightly as possible. In these configurations, the magnetization only has to drop to zero on lines or points, if at all. Considering that it is the competition between phase and amplitude fluctuations that either stabilizes

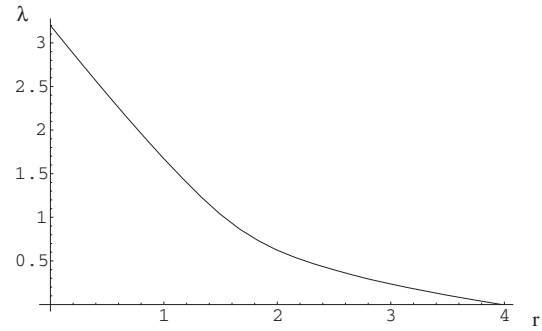


FIG. 2. Amplitude function $\lambda(r)$ which minimizes Eq. (7) using the directional dependence [Eq. (6)], the stabilizing term h_1 (with $\xi = -6.5$, $\eta = 5$), and the boundary condition $\lambda(r) = 0$ for $r > R$. Here, $q = 0.38q_0$ and $R = 3.98$ are free variational parameters where $q_0 = 1/2$ is the helix wave vector. The resulting free energy gain per length is given by $f^{\text{cyl}} = -0.21$.

double-twist structures or not, it can be expected that crystalline arrangements of the helices can exist even in parameter regimes where single cylinders are unstable.

The possible crystalline structures are subject to the condition that the magnetization matches where cylinders touch in order to avoid discontinuities in the magnetization. This condition is much more restrictive for ferromagnets compared to liquid crystals.⁴ We have found⁸ only two allowed structures constructed as networks of double-twist cylinders: a square and a cubic lattice, see Fig. 3. The square lattice is invariant with respect to rotations by multiples of $\pi/2$ around the z axis, translations along the z axis, as well as a translation by $a(\frac{1}{2}, \frac{1}{2}, 0)$ combined with time reversal ($\mathbf{M} \rightarrow -\mathbf{M}$). In this structure, the magnetization has to go to zero on the line $(\frac{a}{2}, 0, z)$ and symmetry-equivalent lines. The symmetry transformations that leave the second structure (cubic lattice) invariant are cyclic permutations of the axes and a translation by $a(\frac{1}{2}, \frac{1}{2}, \frac{1}{2})$ combined with time reversal. In this structure, the magnetization vanishes only at $a(\frac{1}{8}, \frac{5}{8}, \frac{3}{8})$, $a(\frac{3}{8}, \frac{3}{8}, \frac{3}{8})$, and symmetry-equivalent points in the unit cell.

We calculated the free energy density of these structures by means of a variational ansatz for the amplitude of a single double-twist cylinder:

$$\lambda(r) = y_0 \cdot (r_0 - r) e^{-r/r_1} \Theta(r_0 - r), \quad (8)$$

where y_0 , r_1 , and the double-twist wave vector q are variational parameters. This ansatz is based on the numerics for a single cylinder. The cylinders were then arranged in crystals, as shown in Fig. 3. The cutoff $r_0 \approx \sqrt{5}\pi/(2q)$ was chosen for convenience to avoid the tiny overlap of cylinders that are far apart within the calculation.

A phase diagram as a function of the remaining three free parameters can now be computed. Here, we set η to a fixed value, assuming that it is the least susceptible to variations of external pressure, and established the phase diagram as a function of the two remaining free parameters. The result for $\eta = 0.05$ can be seen in Fig. 4.

One immediately notices that there is no parameter regime in which the square lattice shown in Fig. 3(a) has the

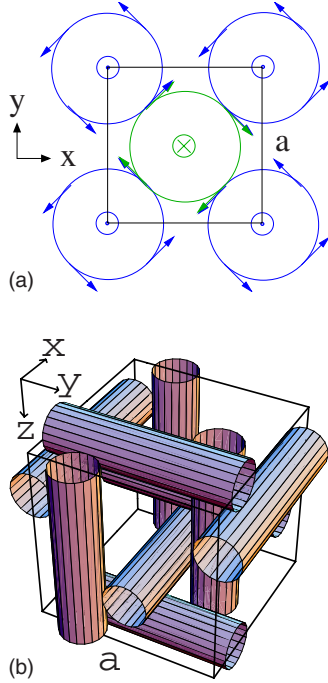


FIG. 3. (Color online) Crystalline structures built from double-twist cylinders: (a) Unit cell of the square lattice of double-twist cylinders in the x - y plane. The magnetization on the cylinder axes, as well as at the points where cylinders touch, is shown explicitly. (b) Unit cell of the cubic lattice of double-twist cylinders. At the points where cylinders touch, the magnetization has twisted to an angle of 45° from the cylinder axis.

lowest free energy density; this is also true for different values of η not shown here. While the filling fraction of double-twist regions is certainly larger in the square lattice than in the cubic structure, the magnetization in the cubic crystal only has to go to zero at points and not on lines, as it is the case for the square lattice. Furthermore, in the cubic lattice, the magnetization only has to twist outward by 45° until cylinders touch, compared to 90° in the case of the square lattice (see Fig. 3). These factors conspire to make the free energy of the cubic structure even lower than that of the square lattice. Within our variational ansatz, we find that the transition from the crystalline to the isotropic phase is very

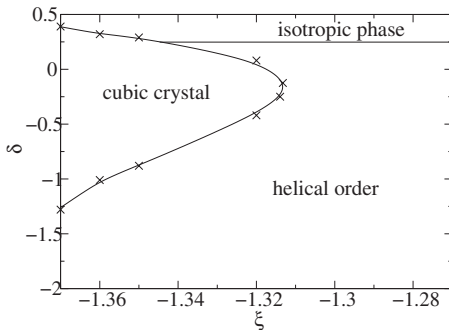


FIG. 4. Phase diagram for $\eta=0.05$. In addition to the helical and the isotropic phases, there is a parameter range where the cubic lattice of double-twist cylinders minimizes the free energy.

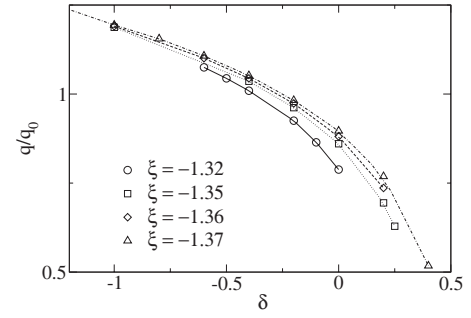


FIG. 5. Ratio of double-twist wave vector q [see Eq. (6)] versus helix wave vector q_0 [see Eq. (4)] for $\eta=0.05$: q/q_0 varies considerably but remains of order 1 in the parameter region where the cubic crystal is stable.

weakly first order [the relevant free energy differences are less than 0.02 in units of Eq. (7)]. Note, however, that our analysis might break down close to the transition, as one enters the high-chirality regime, see above.

Since the double-twist wave vector q is now also a variational parameter, it is no longer necessarily identical to the helix wave vector q_0 . In Fig. 5, we show that q depends considerably on the microscopic parameters but remains of order q_0 .

What signal can these structures be expected to produce in neutron scattering experiments? As for any crystal, peaks in neutron scattering originate from the lattice structure itself, and the configuration of the magnetization within the Wigner-Seitz cell only enters in the shape of form factors. The lattice constants are functions of the double-twist wave vector and determined by the requirement that the magnetization has to match where cylinders touch. For the square lattice, one obtains $a=\sqrt{2}\pi/q$, and for the cubic lattice $a=2\pi/q$.

In neutron scattering, higher-order Bragg peaks can be also expected to be generated by the lattice structures. The elastic scattering cross section⁹ can be calculated from a Fourier transform of the magnetization:

$$\left(\frac{d\sigma}{d\Omega}\right)_{el} \propto |\hat{\mathbf{k}} \times [\mathbf{M}(\mathbf{k}) \times \hat{\mathbf{k}}]|^2. \quad (9)$$

In order to compare with experimental data, the quantities of interest are the positions of the Bragg peaks and the relative intensities of the Bragg peaks.

For the square lattice, normalizing intensities to give unity for the first reflection with Miller indices $\langle 10 \rangle$, the $\langle 21 \rangle$ and $\langle 30 \rangle$ reflections have intensities of 0.08 and 0.01, respectively. The invariance of the square lattice with respect to a translation by $a(\frac{1}{2}, \frac{1}{2})$ combined with $\mathbf{M} \rightarrow -\mathbf{M}$ constrains all Bragg peaks $\langle hk \rangle$ with $h+k=2n$ to vanish. In the case of the square lattice, the lowest order reflexes already account for 84% of the total intensity.

For the cubic lattice, assuming that the lowest Bragg peak, i.e., the $\langle 100 \rangle$ peak, has intensity 1.0, the $\langle 210 \rangle$ and $\langle 300 \rangle$ peaks have relative intensities of 0.17 and 0.03. The $\langle 110 \rangle$ and $\langle 200 \rangle$ peaks vanish for symmetry reasons, while the $\langle 111 \rangle$ peak vanishes as a consequence of our ansatz based

on a linear combination of cylinders in the x , y , and z directions and should really be nonzero as allowed by symmetry. Our approach suggests, however, that these peaks have small weight. The $\langle 100 \rangle$ peaks of the cubic lattice only represent 46% of the total scattering intensity I_{cubic} . The $\langle 100 \rangle$, $\langle 210 \rangle$, and $\langle 300 \rangle$ peaks of the cubic lattice add up to 79% of I_{cubic} .

Anisotropic terms that orient the helix also act on the crystalline structures and determine their orientation with respect to the crystal lattice of the substance. For the square lattice, where all cylinders are arranged in parallel, using Eq. (3) for $B_1=B_2=0$, $B_3 \neq 0$, we find that weak anisotropic terms align the cylinder axes parallel to the preferred direction of the helix vector, i.e., either in the $\langle 111 \rangle$ or $\langle 100 \rangle$ direction, depending on the sign of B_3 . However, the orientation of the crystal in the perpendicular direction is not affected to leading order by the anisotropy term, but higher-order terms would lock a perfect crystal. Motivated by the “partial order” observed in the high-pressure phase of MnSi (see Introduction), we investigate the expected signature in neutron scattering assuming that these higher-order terms are not effective. In this case, the square lattice will produce rings in planes normal to the $\langle 111 \rangle$ direction (the orientation of the helix in the low-pressure phase). These rings intersect to produce maxima in the $\langle 110 \rangle$ direction on a circle with radius $\sqrt{2}q$ in reciprocal space. For parameters with $\sqrt{2}q \approx q_0$, this is consistent with the observed signatures³ in neutron scattering. Note, however, that at least within our model, the square lattice never has the lowest energy.

In Ref. 5, it was argued that an amorphous texture of parallel cylinders (which the authors called skyrmions) aligned preferentially along the $\langle 111 \rangle$ direction would also produce such rings. However, such a scenario would not explain the resolution limited width in the radial direction, i.e., at least on length scales of 2000 Å, the square crystal would have to remain intact.

In the case of the cubic lattice, the numerical calculation of the free energy density shows that for $B_3 > 0$, the anisotropic terms are minimized if one of the axes of the cubic lattice is $\|(1/\sqrt{2}, 1/\sqrt{2}, 0)\|$ and the other axes are $\|(-1/2, 1/2, 1/\sqrt{2})\|$ and $\|(1/2, -1/2, 1/\sqrt{2})\|$, respectively. While such structures would produce peaks in the $\langle 110 \rangle$ direction (as observed in the high-pressure phase of MnSi), one expects also considerable intensity rather close to $\langle 111 \rangle$ [as, e.g., $(-1/2, 1/2, 1/\sqrt{2})$ differs only by about 10° from (-111)]. Experimentally, however, one observes a minimum of the intensity in the $\langle 111 \rangle$ direction. For $B_1=B_2=0$, $B_3 < 0$, the system would prefer to align the cubic structure with the crystal lattice of MnSi.

Binz *et al.*⁶ have argued that the Bragg peaks in neutron scattering should be smeared out because the magnetization

has a varying amplitude, and is therefore susceptible to interactions with nonmagnetic impurities. The same argument would apply for the crystalline structures presented in this paper.

IV. CONCLUSIONS

In conclusion, we have constructed “blue phases” in chiral ferromagnets. Is it likely that these blue phases are realized in MnSi? The signatures in neutron scattering seem to be consistent with the square structure (also considered in Ref. 5), which is, however, never the ground state within the models that we considered. Our results suggest that the intensity in neutron scattering is located on rings intersecting in the $\langle 110 \rangle$ direction. It would be interesting to check experimentally whether the intensity distribution arising from such a picture fits quantitatively.

In the case of the cubic lattice, the positions of the expected maxima do not match the ones observed. In any case, the smoking gun experiment to detect crystalline structures would be the observation of higher-order Bragg peaks (this also applies for other structures, e.g., those suggested in Refs. 5 and 6) and we hope that our estimates may guide future experiments in this direction.

However, it is still unclear whether the partially ordered state of MnSi is indeed a separate phase. Recent measurements of the thermal expansion coefficient give no trace of a phase transition from the partially ordered state to the isotropic phase.¹⁰ Furthermore, muon spin spectroscopy experiments¹¹ give no evidence for static order in this regime and it remains unclear on which time scales the partial order survives.³

It therefore remains an open question whether distinct phases other than the helical one are present in chiral ferromagnets that are currently investigated experimentally. In fact, the partially ordered phase in MnSi might be more analogous to the blue phase III than to blue phases I and II. While the precise structure of the blue phase III is not completely clear, it seems to show some type of crystalline short range order but is a liquid on long length scales.^{12,13} Therefore, it has been conjectured¹⁴ that an amorphous arrangement of double-twist cylinders is relevant for this blue phase III in liquid crystals—this might also be true^{3,5,15} for the partially ordered phase in MnSi.

ACKNOWLEDGMENTS

We thank B. Binz, C. Pfeleiderer, U. K. Rößler, and A. Vishwanath for useful discussions and the SFB 608 of the DFG for financial support.

¹P. Bak and M. Høgh, J. Phys. C **13**, 881 (1980); O. Nakanishi, A. Yanase, A. Hasegawa, and M. Kataoka, Solid State Commun. **35**, 995 (1980).

²C. Pfeleiderer, S. R. Julian, and G. G. Lonzarich, Nature (London) **414**, 427 (2003).

³C. Pfeleiderer, D. Reznik, L. Pintschovius, H. v. Löhneysen, M. Garst, and A. Rosch, Nature (London) **427**, 227 (2004).

⁴D. C. Wright and N. D. Mermin, Rev. Mod. Phys. **61**, 385 (1989).

⁵U. K. Rößler, A. N. Bogdanov, and C. Pfeleiderer, Nature (London) **442**, 797 (2006); see also supplementary notes.

- ⁶B. Binz, A. Vishwanath, and V. Aji, Phys. Rev. Lett. **96**, 207202 (2006); B. Binz and A. Vishwanath, Phys. Rev. B **74**, 214408 (2006).
- ⁷D. Belitz, T. R. Kirkpatrick, and A. Rosch, Phys. Rev. B **73**, 054431 (2006).
- ⁸Although the three-dimensional structures proposed in Ref. 6 cannot be realized with double-twist cylinders, they nonetheless contain large, clearly identifiable regions that exhibit double-twist structures.
- ⁹G. L. Squires, *Introduction to the Theory of Thermal Neutron Scattering* (Dover, New York, 1996).
- ¹⁰C. Pfeleiderer, P. Böni, T. Keller, U. K. Röbner, and A. Rosch, Science **316**, 1871 (2007).
- ¹¹Y. J. Uemura, T. Goko, I. M. Gat-Malureanu, J. P. Carlo, P. L. Russo, A. T. Savici, A. Aczel, G. J. MacDougall, J. A. Rodriguez, G. M. Luke, S. R. Dunsiger, A. McCollam, J. Arai, Ch. Pfeleiderer, P. Böni, K. Yoshimura, E. Baggio-Saitovitch, M. B. Fontes, J. Larrea, Y. V. Sushko, and J. Sereni, Nat. Phys. **3**, 29 (2007).
- ¹²H.-S. Kitzerow and C. E. Bahr, *Chirality in Liquid Crystals* (Springer, Berlin, 2001).
- ¹³E. P. Koistinen and P. H. Keyes, Phys. Rev. Lett. **74**, 4460 (1995).
- ¹⁴R. M. Hornreich, M. Kugler, and S. Shtrikman, Phys. Rev. Lett. **48**, 1404 (1982).
- ¹⁵S. Tewari, D. Belitz, and T. R. Kirkpatrick, Phys. Rev. Lett. **96**, 047207 (2006).